

Original Article

***UHRF1* knockdown induces cell cycle arrest and apoptosis in breast cancer cells through the ZBTB16/ANXA7/Cyclin B1 axis**

Di Liu¹, Qin Du¹, Yuxuan Zhu¹, Yize Guo¹, and Ya Guo^{2,*}

¹The Comprehensive Breast Care Center, the Second Affiliated Hospital of Xi'an Jiaotong University, Xi'an 710004, China, and ²Department of Radiation Oncology, the Second Affiliated Hospital of Xi'an Jiaotong University, Xi'an 710004, China

*Correspondence address. Tel: +86-29-87679691; E-mail: guoya_gy8569851@163.com

Received 17 November 2023 Accepted 29 March 2024

Abstract

Ubiquitin-like containing PHD and RING finger domains 1 (*UHRF1*) is involved in tumorigenicity through DNA methylation in various cancers, including breast cancer. This study aims to investigate the regulatory mechanisms of *UHRF1* in breast cancer progression. Herein, we show that *UHRF1* is upregulated in breast cancer tissues and cell lines as measured by western blot analysis and immunohistochemistry. Breast cancer cells are transfected with a *UHRF1* overexpression plasmid (pcDNA-*UHRF1*) or short hairpin RNA targeting *UHRF1* (sh-*UHRF1*), followed by detection of cell proliferation, invasion, apoptosis, and cell cycle. *UHRF1* overexpression promotes proliferation and invasion and attenuates cell cycle arrest and apoptosis in breast cancer cells, while *UHRF1* knockdown shows the opposite effect. Moreover, methylation-specific PCR and ChIP assays indicate that *UHRF1* inhibits zinc finger and BTB domain containing 16 (*ZBTB16*) expression by promoting *ZBTB16* promoter methylation via the recruitment of DNA methyltransferase 1 (*DNMT1*). Then, a co-IP assay is used to verify the interaction between *ZBTB16* and the annexin A7 (*ANXA7*) protein. *ZBTB16* promotes *ANXA7* expression and subsequently inhibits Cyclin B1 expression. Rescue experiments reveal that *ZBTB16* knockdown reverses the inhibitory effects of *UHRF1* knockdown on breast cancer cell malignancies and that *ANXA7* knockdown abolishes the inhibitory effects of *ZBTB16* overexpression on breast cancer cell malignancies. Additionally, *UHRF1* knockdown significantly inhibits xenograft tumor growth *in vivo*. In conclusion, *UHRF1* knockdown inhibits proliferation and invasion, induces cell cycle arrest and apoptosis in breast cancer cells via the *ZBTB16/ANXA7/Cyclin B1* axis, and reduces xenograft tumor growth *in vivo*.

Key words breast cancer, cell cycle, *UHRF1*, DNA methylation, the *ZBTB16/ANXA7/Cyclin B1* axis

Introduction

Breast cancer is the most common cancer in women worldwide and is the second leading cause of cancer-related death among women [1]. Currently, clinical therapeutic strategies include surgical resection, chemotherapy, adjuvant radiotherapy, and targeted biotherapy [2]. Although significant improvements have rapidly been made in the management of breast cancer, the outcomes remain seriously unsatisfactory owing to the increasing incidence rate and tumor recurrence and metastasis [3]. Thus, there is an urgent need to clarify the molecular mechanism of breast cancer progression and formulate more effective clinical treatment strategies.

Ubiquitin-like containing PHD and RING finger domains 1

(*UHRF1*), also known as ICBP90 in humans and Np95 in mice, has been identified as a multidomain protein. It has been reported that *UHRF1* is upregulated in multiple cancers, and its dysregulation is associated with proliferation, cell cycle arrest and apoptosis in cancer cells. For instance, *UHRF1* is elevated in cutaneous squamous cell carcinoma (cSCC), and knockdown of *UHRF1* attenuates cSCC cell proliferation, migration, and invasion, leading to G2/M cell cycle arrest and increased apoptosis [4]. *UHRF1* expression is upregulated in patients with hepatocellular carcinoma (HCC), while knockdown of *UHRF1* inhibits proliferation and metastasis and induces G2/M cell cycle arrest in HCC cells [5]. *UHRF1* has also been identified as an important epigenetic factor that regulates DNA methylation. The SET and RING-associated

(SRA) domain of UHRF1 has been proven to be required for the maintenance of DNA methyltransferase 1 (DNMT1)-mediated DNA methylation [6]. Accumulating evidence indicates that UHRF1 is involved in tumorigenicity by promoting DNA promoter methylation and subsequently silencing tumor suppressor genes. It was found that UHRF1 induces DNMT1-mediated promoter methylation and subsequently downregulates the expressions of tumor suppressor genes, thus inhibiting cell cycle arrest and apoptosis in cervical cancer [7]. UHRF1 facilitates gastric cancer proliferation and growth *in vitro* and *in vivo* by mediating hypermethylation of several tumor suppressor genes [8]. Notably, it was previously reported that UHRF1 promotes the proliferation, invasion and migration of breast cancer cells [9]. Moreover, short hairpin RNA (shRNA) lentiviral system-mediated *UHRF1* knockdown inhibits breast cancer cell proliferation [10], indicating that UHRF1 may serve as a promising therapeutic target for breast cancer. However, the regulatory mechanisms of UHRF1 in breast cancer progression have not been fully characterized.

Zinc finger and BTB domain containing 16 (ZBTB16), also known as promyelocytic leukemia zinc finger (PLZF) or zinc finger protein 145 (ZFP145), is a member of the zinc finger and BTB/POZ domain-containing family of proteins (ZBTBs). Recent studies have shown that ZBTB16 participates in various major biological processes, such as hematopoiesis, spermatogenesis, stem cell maintenance, tumor suppression and immune regulation [11,12]. Downregulation of ZBTB16 has been detected in various cancers and malignant cell lines. ZBTB16 is significantly downregulated in HCC samples at both the mRNA and protein levels and may be a potential biomarker for the diagnosis of HCC [13]. ZBTB16 was also found to be downregulated in malignant mesothelioma cell lines compared with nonmalignant mesothelial cells, and downregulation of ZBTB16 may contribute to malignant mesothelioma pathogenesis by promoting cell survival [14]. Importantly, it was reported that ZBTB16 is downregulated in breast cancer cell lines, which is associated with its promoter hypermethylation, and restoration of ZBTB16 expression inhibits tumorigenesis [15]. Thus, whether the promoter hypermethylation of ZBTB16 is correlated with the upregulation of UHRF1 in breast cancer needs to be investigated.

In the present study, we investigated the effects of UHRF1 on breast cancer progression *in vivo* and *in vitro* and further explored the regulatory mechanisms of the UHRF1/ZBTB16 axis in regulating breast cancer progression, aiming to provide a reliable target for breast cancer treatment.

Materials and Methods

Clinical samples

A total of 30 paired breast cancer tissues and matched adjacent normal tissues were collected from breast cancer patients admitted to the Department of Oncology, the Second Affiliated Hospital of Xi'an Jiaotong University (Xi'an, China). No patients underwent chemotherapy, radiotherapy, immunotherapy, or other anticancer treatments before surgery. All tissue samples were immediately frozen in liquid nitrogen and then stored at -80°C . This study was approved by the Ethics Committee of Xi'an Jiaotong University, and written informed consent was obtained from each participant.

Cell culture and transfection

Breast cancer cell lines (BT-474, MDA-MB-231, MCF-7, and SKBR3) and the human normal breast epithelial cell line MCF-10A were

obtained from the American Type Culture Collection (ATCC; Manassas, USA). The cells were cultured in Dulbecco's modified Eagle's medium (DMEM; Gibco, Grand Island, USA) supplemented with 10% fetal bovine serum (FBS; Gibco) and a 1% penicillin/streptomycin mixture (Gibco) in a humidified atmosphere with 5% CO_2 at 37°C .

Overexpression plasmids for UHRF1 (pcDNA-UHRF1) and ZBTB16 (pcDNA-ZBTB16), short hairpin RNAs targeting UHRF1 (sh-UHRF1, 5'-GATCCGACGCCAGGACCTCATTCCTCGAGCCTTACTCCAGGACCGCAGTTTTTC-3'), ZBTB16 (sh-ZBTB16, 5'-CCGGGAATGCACTTACTGGCTCATTCTCGAGAATGAGCCAGTAAGTGCACTCTTTTGTG-3') and ANXA7 (sh-ANXA7, 5'-GATCCGTGAGAATTGAGTGGGAATTGGTGAGTTAAGACTGTTTTTC-3'), and their corresponding negative controls (vector and sh-NC, 5'-GATCCGACACCTACGCAAAACCCTCTCGAGTCCCAAAACGCATCCACAGTTTTTC-3') were obtained from RiboBio (Guangzhou, China). Breast cancer cells were seeded in 6-well plates, and cell transfection was carried out by using Lipofectamine 3000™ reagent (Invitrogen, Carlsbad, USA) according to the manufacturer's instructions. The cells were collected at 48 h posttransfection for subsequent experiments.

Western blot analysis

Total protein was extracted from tissues or cell lines by using RIPA lysis buffer (HY-K1001; MedChemExpress, Shanghai, China). The protein concentrations were determined using BCA reagent (Millipore, Billerica, USA). Equal amounts of protein samples were separated by 10% SDS-PAGE, and the protein bands were transferred to polyvinylidene difluoride (PVDF) membranes (Millipore) at 300 mA for 2 h. The membranes were then blocked with 5% nonfat milk for 1 h at room temperature and incubated overnight at 4°C with the following primary antibodies: rabbit monoclonal anti-UHRF1 antibody (1:500, ab213223; Abcam, Cambridge, UK), mouse monoclonal anti-ZBTB16 antibody (1:400, ab104854; Abcam), rabbit monoclonal anti-ANXA7 antibody (1:600, ab197586; Abcam), rabbit monoclonal anti-Cyclin B1 antibody (1:800, ab181593; Abcam), and rabbit polyclonal anti-GAPDH antibody (1:1000, ab9485; Abcam). The membranes were incubated with horseradish peroxidase (HRP)-conjugated goat anti-rabbit IgG (1:2000, ab6721; Abcam) or goat anti-mouse IgG (1:2000, ab6789; Abcam) for 1 h at room temperature. After extensive washing, the protein bands were visualized with an enhanced chemiluminescence (ECL) detection kit (Pierce Biotechnology, Rockford, USA) and analyzed with ImageJ software (National Institutes of Health, Bethesda, USA) in a gel imaging analysis system. GAPDH was used as a loading control.

RNA extraction and RT-qPCR

Total RNA was extracted from tissues or cells by using TRIzol reagent (Invitrogen). The RNA concentration was evaluated by using a spectrophotometer (Bio-Rad, Hercules, USA). Total RNA was reverse transcribed into cDNA by using the PrimeScript RT Reagent kit (TaKaRa, Dalian, China). Then, real-time PCR was performed to determine ZBTB16 mRNA expression by using SYBR Premix Ex Taq II (TaKaRa) on an ABI 7500 Real-Time PCR System (Applied Biosystems, Foster City, USA) under the following conditions: 95°C for 1 min, 95°C for 20 s, 56°C for 10 s and 72°C for 15 s for 35 cycles. *ZBTB16* mRNA expression was normalized to that of glyceraldehyde 3-phosphate dehydrogenase (*GAPDH*). The

relative expression was calculated by the $2^{-\Delta\Delta CT}$ method. The primers used were as follows: *ZBTB16* (forward: 5'-GAGCTTCCTGATAACGAGGCTG-3', reverse: 5'-AGCCGCAAACCTATCCAGGAACC-3') and *GAPDH* (forward: 5'-TCCACCACCCTGTTGCTGTA-3', reverse: 5'-ACCACAGTCCATGCCATCAC-3').

Cell counting kit-8 (CKK-8) assay

Cell proliferation was determined by using a Cell Counting Kit-8 (CKK-8; Dojindo Laboratories, Kumamoto, Japan). Briefly, the transfected breast cancer cells (1×10^4 cells/well) were seeded into 96-well plates and kept in a humidified atmosphere with 5% CO_2 at 37°C. After incubation for 0, 24, 48 and 72 h, 10 μ L of CKK-8 solution was added to each well prior to incubation for 2 h at 37°C. Then, the absorbance of each well at 450 nm was measured by using a microplate reader (Bio-Rad).

EdU assay

Totally, 4×10^3 cells were seeded in 96-well plates and kept in a humidified atmosphere with 5% CO_2 at 37°C. After incubation for 48 h, 10 μ M EdU (Dojindo Laboratories) was added to each well prior to incubation for 2 h at 37°C. The cells were then fixed with 4% Paraformaldehyde Fixation and permeabilized with 0.5% Triton X-100 solution for 10 min. After being washed with PBS for 5 min, the cells were stained with Apollo® solution (Millipore) and the nuclei were stained with Hoechst33342 (Invitrogen). The cells were observed under a fluorescence microscope (Olympus, Tokyo, Japan).

Transwell invasion assay

Cell invasion was evaluated by Transwell assay using a specific Transwell chamber (8 μ m pore size; Millipore) precoated with Matrigel matrix (BD Biosciences, San Jose, USA). Briefly, a total of 1×10^5 breast cancer cells in DMEM were seeded into the upper chamber, while DMEM containing 10% FBS was added to the lower chamber. After incubation for 24 h at 37°C, the cells in the upper chamber were removed by using a cotton swab, and the invaded cells in the bottom chamber were fixed and stained with 0.1% crystal violet for 15 min. The number of invaded cells in five randomly selected visual fields was counted under an inverted microscope (Olympus).

Cell apoptosis analysis

Flow cytometry analysis was performed to measure cell apoptosis by using the Annexin V-FITC Apoptosis Detection kit (Biolegend, San Diego, USA). Briefly, the transfected cells were collected and resuspended in 1 \times binding buffer at a density of 1×10^6 cells/mL and then stained with 5 μ L of Annexin V-FITC and 5 μ L of propidium iodide (PI) for 15 min in the dark at room temperature. Cell apoptosis was detected with a flow cytometer (BD Bioscience) according to the manufacturer's instructions.

Cell cycle analysis

The cell cycle distribution was analyzed by flow cytometry after propidium iodide (PI) staining. Briefly, transfected cells were harvested upon reaching 80% confluence and fixed with ice-cold 70% ethanol at 4°C overnight. The cells were washed with PBS and then treated with PI staining solution in the dark at room temperature for 30 min. Finally, the cell cycle distribution was analyzed by using the flow cytometer, and the percentage of the cells present in each cell cycle phase was determined.

Coimmunoprecipitation (Co-IP) assay

MDA-MB-231 cells were lysed with RIPA lysis buffer, and the supernatant was collected. The supernatant was incubated with anti-UHRF1 or anti-ZBTB16 antibody at 4°C overnight, followed by incubation with 100 μ L of protein A/G agarose beads (TaKaRa) overnight at 4°C. The mixture was centrifuged to collect the agarose bead-antigen-antibody complex. Then, the complex was boiled with loading buffer for 5 min, and the supernatant was collected by centrifugation. Finally, the expression of interacting proteins was analyzed by western blot analysis.

Chromatin immunoprecipitation (ChIP)

The interaction between DNA methyltransferase 1 (DNMT1) and the *ZBTB16* promoter was examined by chromatin immunoprecipitation (ChIP) using an EZ-Magna ChIP TMA kit (Millipore). In brief, BEAS-2B cells were fixed with 1% formaldehyde for 10 min to generate DNA-protein cross-links. Then, the cells were lysed in lysis buffer, and chromatin fragments at 200–1000 bp were collected by sonication on ice for 3 min. The chromatin fragments were incubated with anti-DNMT1 (ab13537; Abcam) or IgG (ab10948; Abcam) for immunoprecipitation at 4°C overnight. An aliquot of cell lysates served as an input DNA control. The DNA-protein complex was precipitated with Protein Agarose/Sepharose (TaKaRa). The precipitated DNA was purified and subjected to RT-qPCR analysis.

Methylation specific PCR (MSP)

The methylation levels of the *ZBTB16* promoter region were detected by methylation-specific PCR (MSP). DNA was extracted from MDA-MB-231 cells by using a genomic DNA extraction kit (Tiangen Biochemistry Technology, Beijing, China) and then subjected to bisulfite modification with an EpiTect Bisulfite kit (Qiagen, Dusseldorf, Germany) according to the manufacturer's instructions. The MSP reaction was conducted using AmpliTaq-Gold DNA Polymerase (Applied Biosystems) on an ABI 7500 quantitative PCR System (Applied Biosystems). Then, the reaction products were analyzed by agarose gel electrophoresis and imaged with a gel electrophoresis imaging analysis system. The following MSP primers for *ZBTB16* were used: methylated (forward: 5'-AAGAGGCGTATCGTTTAGCG-3', reverse: 5'-CCCAACGACCGAA TAACCG-3') and unmethylated (forward: 5'-GGAAGAGGTGATT GTTTAGTGAG-3', reverse: 5'-AACCCAACAACCAATAACCAAA-3').

Xenograft assay

Four-week-old female BALB/c nude mice were provided by the animal experimental center of Xi'an Jiaotong University. Mice were randomly divided into two groups: the sh-NC group and the sh-UHRF1 group ($n=8$ per group). MDA-MB-231 cells (0.2 mL, 2×10^6) transfected with sh-NC or sh-UHRF1 were injected subcutaneously into the right axilla of the mice. Tumor volumes were measured every 7 days for 28 consecutive days after injection. The nude mice were euthanized on day 28, and the tumor tissues were collected and weighed. The animal experiments were conducted in accordance with the Ethics Committee of Xi'an Jiaotong University.

Immunohistochemistry (IHC) assay

Tumor tissues were cut into 4- μ m-thick sections, and then the tissue sections were fixed with 4% formaldehyde overnight and embedded in paraffin. After deparaffinization and hydration, the

sections were pretreated with sodium citrate buffer in a microwave oven for antigen retrieval and then blocked with goat serum for 1 h at room temperature. The sections were then incubated with primary antibodies against UHRF1, ZBTB16 or ANXA7 overnight at 4°C and then with HRP-conjugated goat anti-rabbit IgG (ab6721; Abcam) at 37°C for 1 h. Subsequently, the sections were stained with a diaminobenzidine (DAB) kit and observed under a light microscope (Olympus).

Statistical analysis

Data analysis was performed with SPSS version 22.0 software. All data from at least three independent experiments are presented as the mean±standard deviation (SD). Student's *t* test was used for comparisons between two groups, and analysis of variance (ANOVA) followed by Tukey's test was used for comparisons among groups. *P*<0.01 was considered to indicate statistical significance.

Results

UHRF1 is upregulated in breast cancer tissues and cell lines

To investigate whether UHRF1 is involved in the progression of breast cancer, we retrieved the Gene Expression Profiling Interactive Analysis (GEPIA) database, which showed that UHRF1

expression was upregulated in breast cancer tissues compared with normal tissues (Figure 1A). Then, we detected the protein expression of UHRF1 in tumor tissues and matched adjacent tissues from breast cancer patients by using IHC assay and western blot analysis. The protein expression of UHRF1 was upregulated in breast cancer tissues compared with that in matched adjacent tissues (Figure 1B–D). Moreover, we also found that UHRF1 was upregulated in breast cancer cell lines (BT-474, MDA-MB-231, MCF-7, and SKBR3) compared with that in the human normal breast epithelial cell line MCF-10A (Figure 1E). Thus, we speculated that UHRF1 might be involved in breast cancer progression.

UHRF1 knockdown induces cell cycle arrest and apoptosis in breast cancer cells

To explore the role of UHRF1 in the progression of breast cancer, MDA-MB-231 and MCF-7 cells were transfected with pcDNA-UHRF1 and sh-UHRF1, respectively. Western blot analysis revealed that transfection with pcDNA-UHRF1 upregulated the protein expression of UHRF1, while transfection with sh-UHRF1 downregulated the protein expression of UHRF1 in MDA-MB-231 cells (Figure 2A) and MCF-7 cells (Supplementary Figure S1A). CCK-8 assay indicated that UHRF1 overexpression significantly promoted proliferation, while UHRF1 knockdown inhibited proliferation in MDA-MB-231 cells (Figure 2B) and MCF-7 cells (Supplementary

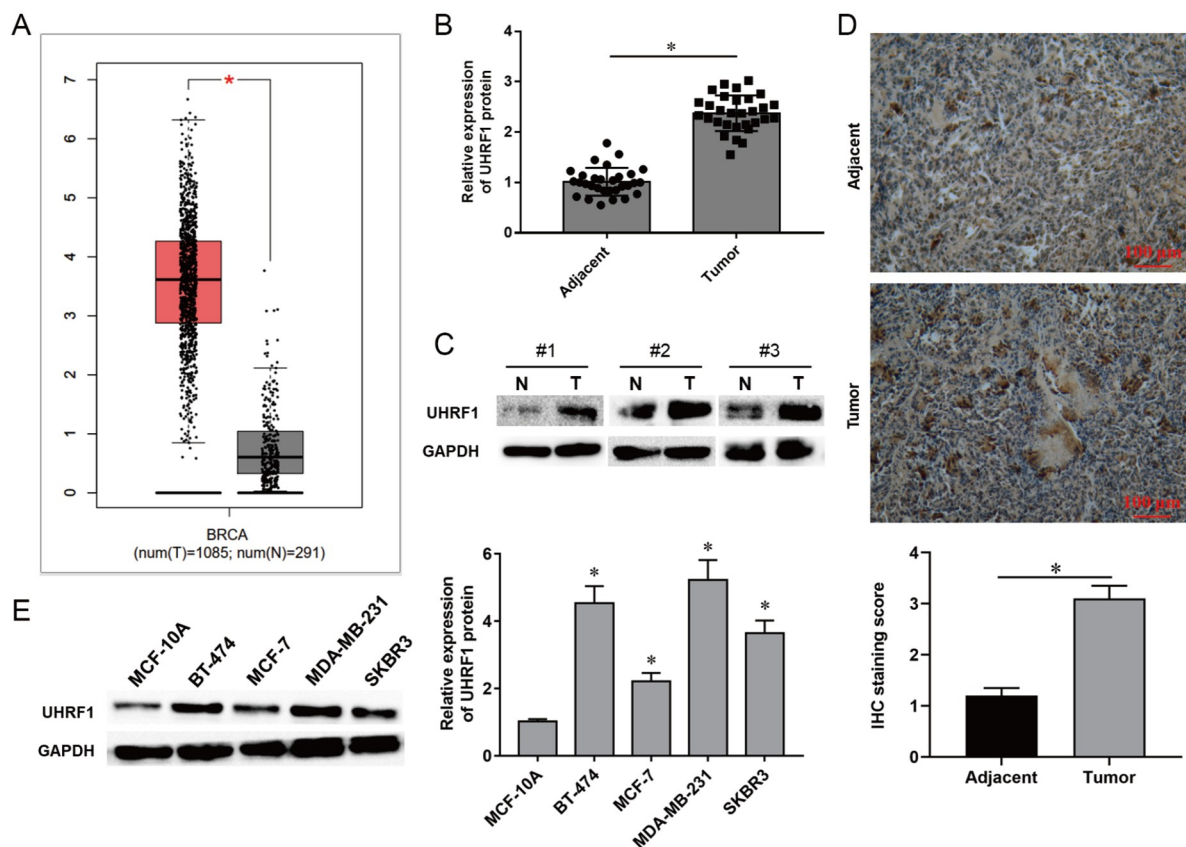


Figure 1. UHRF1 is upregulated in breast cancer tissues and cell lines (A) Relative expression of UHRF1 in breast cancer was retrieved from the Gene Expression Profiling Interactive Analysis (GEPIA) database. (B,C) The relative expression of UHRF1 in breast cancer tissues and matched adjacent tissues was measured by western blot analysis (*n*=30 per group). (D) Relative expression of UHRF1 in breast cancer tissues and matched adjacent tissues was measured by immunohistochemistry (×100). (E) The relative expression of UHRF1 in breast cancer cell lines (BT-474, MDA-MB-231, MCF-7, and SKBR3) and the human normal breast epithelial cell line MCF-10A was measured via western blot analysis. Data are presented as the mean±SD from at least three replicate experiments. **P*<0.01.

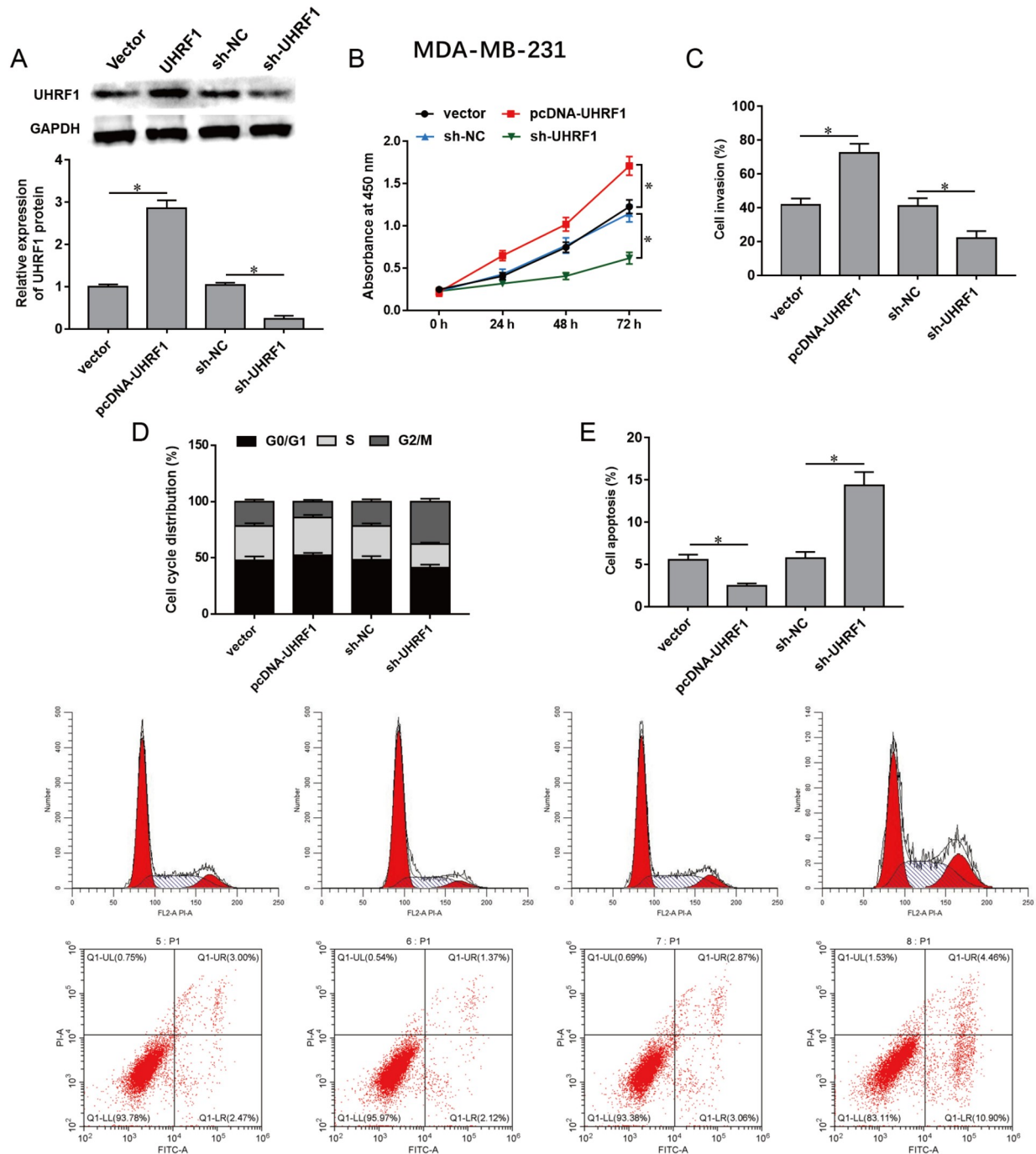


Figure 2. The effects of UHRF1 on proliferation, invasion, cell cycle progression and apoptosis in breast cancer cells MDA-MB-231 cells were transfected with pcDNA-UHRF1 (1 μ g/mL), sh-UHRF1 (1 mL, 10^{10} PFU/mL), or their corresponding negative controls. (A) The protein expression of UHRF1 in MDA-MB-231 cells was measured by western blot analysis at 48 h post-transfection. (B) CCK-8 assay was performed to detect cell proliferation. (C) Transwell assays were used to detect cell invasion. (D) The cell cycle distribution was analyzed by flow cytometry. (E) Cell apoptosis was measured by flow cytometry. Data are presented as the mean \pm SD from at least three replicate experiments. * P < 0.01.

Figure S1B). Transwell assay showed that UHRF1 overexpression promoted invasion, while UHRF1 knockdown inhibited invasion in MDA-MB-231 cells (Figure 2C) and MCF-7 cells (Supplementary Figure S1C). Moreover, UHRF1 overexpression reduced the percentage of MDA-MB-231 cells in the G2/M phase, while UHRF1 knockdown increased the percentage of MDA-MB-231 cells in the G2/M phase (Figure 2D) and MCF-7 cells in the G2/M phase

(Supplementary Figure S1D), indicating that UHRF1 plays a role in breast cancer cell cycle arrest. Additionally, UHRF1 overexpression attenuated cell apoptosis, while UHRF1 knockdown promoted apoptosis in MDA-MB-231 cells (Figure 2E) and MCF-7 cells (Supplementary Figure S1E). These data indicated that UHRF1 has a suppressive effect on cell cycle arrest and apoptosis in breast cancer cells.

UHRF1 promotes *ZBTB16* promoter methylation by recruiting DNMT1

It was reported that *ZBTB16* is downregulated in breast cancer cell lines, which is correlated with its promoter methylation status [15]. UHRF1 is an important epigenetic regulator that recruits DNMT1 to maintain DNA methylation [16]. To investigate whether *ZBTB16* expression is regulated by UHRF1, we first verified the interaction between UHRF1 and DNMT1 in MDA-MB-231 cells through Co-IP assay (Figure 3A). We found that CpG islands existed in the *ZBTB16* promoter region (Figure 3B) by using the MethPrimer (<http://www.urogene.org/cgi-bin/methprimer/methprimer.cgi>) website. Furthermore, ChIP results indicated that DNMT1 was enriched in the promoter region of *ZBTB16*, and UHRF1 overexpression promoted the enrichment of DNMT1 in the *ZBTB16* promoter (Figure 3C). MSP-PCR was further performed to analyze the methylation level of the *ZBTB16* promoter in MDA-MB-231 cells. As shown in Figure 3D, UHRF1 overexpression enhanced the *ZBTB16* methylation level, while UHRF1 knockdown and treatment with a DNA methyltransferase inhibitor (5-Aza-CdR) both reduced the *ZBTB16* methylation level in MDA-MB-231 cells. Subsequently, RT-qPCR and western blot analyses illustrated that UHRF1 overexpression significantly decreased the mRNA and protein expression levels of *ZBTB16*, while UHRF1 knockdown increased the expression of *ZBTB16* in MDA-MB-231 cells (Figure 3E,F). Then, we performed preliminary explorations of the demethylation of the *ZBTB16* promoter. We evaluated the coexpression of *ZBTB16* and several major demethylases using the TCGA database and found that *ZBTB16* expression is positively associated with TET2 level (Supplementary Figure S2A).

Moreover, we found that there is a potential binding site for TET2 on the *ZBTB16* promoter through motif searching (Supplementary Figure S2B,C) and demonstrated that TET2 (not TET1 and TET3) directly binds to the *ZBTB16* promoter via ChIP-qPCR assay (Supplementary Figure S2D). Based on the current findings, we believe that TET2 is likely the DNA demethylase involved in this process. Collectively, our results demonstrated that UHRF1 reduces *ZBTB16* expression by promoting *ZBTB16* promoter methylation by recruiting DNMT1.

UHRF1 knockdown induces cell cycle arrest and apoptosis in breast cancer cells by inhibiting *ZBTB16* expression

To explore whether UHRF1 functions in breast cancer progression by regulating *ZBTB16*, MDA-MB-231 cells were transfected with sh-UHRF1 alone or in combination with sh-*ZBTB16*. Western blot analysis indicated that transfection with sh-UHRF1 increased *ZBTB16* expression, while transfection with sh-*ZBTB16* decreased *ZBTB16* expression (Figure 4A). Moreover, UHRF1 knockdown inhibited proliferation (Figure 4B) and invasion (Figure 4C) in MDA-MB-231 cells, while *ZBTB16* knockdown reversed these effects. Flow cytometry analysis revealed that UHRF1 knockdown induced cell cycle arrest at the G2/M phase in MDA-MB-231 cells, and this effect was abolished by *ZBTB16* knockdown (Figure 4D). In addition, UHRF1 knockdown enhanced cell apoptosis, while *ZBTB16* knockdown inhibited apoptosis in MDA-MB-231 cells (Figure 4E). These data indicated that knockdown of UHRF1 induced cell cycle arrest and apoptosis in breast cancer cells by

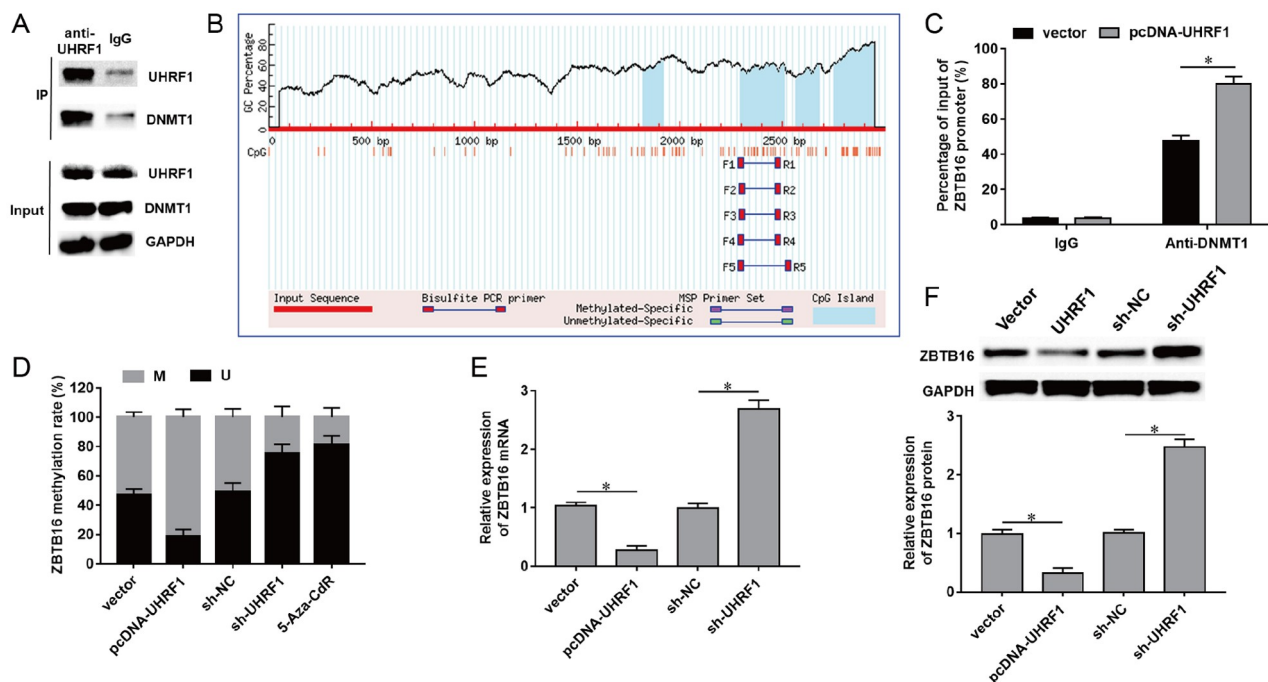


Figure 3. UHRF1 promotes *ZBTB16* promoter methylation by recruiting DNMT1 (A) The interaction between the *ZBTB16* protein and DNMT1 protein was verified by co-IP assay. (B) The distribution of CpG islands within the *ZBTB16* promoter region was analyzed via the MethPrimer website. (C) ChIP assays were performed to detect the enrichment of the DNMT1-bound *ZBTB16* promoter sequence in MDA-MB-231 cells before and after UHRF1 overexpression. (D) MSP was used to detect the methylation level of the *ZBTB16* promoter region in MDA-MB-231 cells before and after UHRF1 overexpression or knockdown and after the addition of the DNA methyltransferase inhibitor 5-Aza-CdR (U, unmethylation; M, methylation; 5-Aza-CdR, 5-Aza-2'-deoxycytidine). (E) MDA-MB-231 cells were transfected with pcDNA-UHRF1, sh-UHRF1 or their corresponding negative controls. The mRNA and protein levels of *ZBTB16* were measured by RT-qPCR and western blot analysis respectively. Data are presented as the mean±SD from at least three replicate experiments. * $P<0.01$.

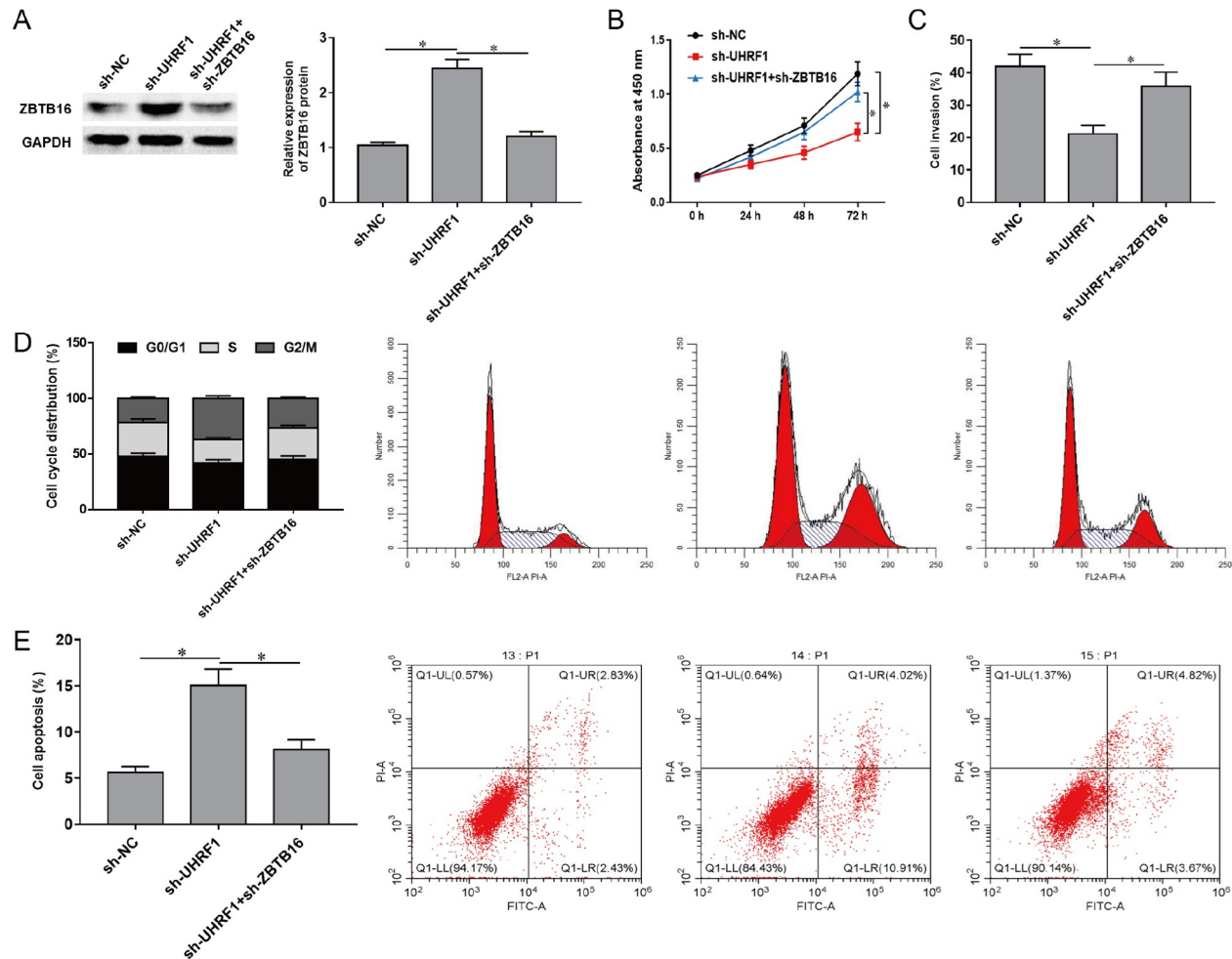


Figure 4. UHRF1 knockdown induces cell cycle arrest and apoptosis in breast cancer cells by inhibiting ZBTB16 expression MDA-MB-231 cells were transfected with sh-UHRF1 (1 mL, 10^{10} PFU/mL) alone or in combination with sh-ZBTB16 (1 mL, 10^{10} PFU/mL). (A) The protein expression of ZBTB16 was measured by western blot analysis at 48 h posttransfection. (B) Cell proliferation was detected by CCK-8 assay. (C) Transwell assays were used to detect cell invasion. (D) Cell cycle distribution was analyzed by flow cytometry. (E) Cell apoptosis was measured by flow cytometry. Data are presented as the mean \pm SD from at least three replicate experiments. * $P < 0.01$.

inhibiting ZBTB16 expression.

ZBTB16 interacts with ANXA7 and positively regulates ANXA7 expression

To further explore the regulatory mechanism of ZBTB16 in breast cancer progression, the potential interacting proteins of ZBTB16 were predicted by using the BioGRID website (<https://thebiogrid.org/>). There was a potential interaction relationship between the ZBTB16 and ANXA7 proteins. Co-IP assays demonstrated that both the ZBTB16 and ANXA7 proteins could be immunoprecipitated by the anti-ZBTB16 antibody but not by IgG in MDA-MB-231 cells, indicating that ZBTB16 can interact with ANXA7 in MDA-MB-231 cells (Figure 5A). MDA-MB-231 cells were transfected with pcDNA-ZBTB16 or sh-ZBTB16, and transfection with pcDNA-ZBTB16 significantly increased ZBTB16 expression, while transfection with sh-ZBTB16 reduced ZBTB16 expression (Figure 5B,C). Western blot analysis indicated that ZBTB16 overexpression promoted ANXA7 protein expression, while ZBTB16 knockdown inhibited ANXA7 protein expression in MDA-MB-231 cells. Furthermore, our results revealed that ZBTB16 overexpression decreased Cyclin B1 protein

expression, while ZBTB16 knockdown promoted Cyclin B1 protein expression in MDA-MB-231 cells (Figure 5B,D,E), indicating that ZBTB16 may mediate the cell cycle through regulating the ANXA7/Cyclin B1 axis.

ZBTB16 induces cell cycle arrest and apoptosis in breast cancer cells by regulating the ANXA7/Cyclin B1 axis

To further investigate the involvement of ANXA7 in ZBTB16-mediated breast cancer progression, MDA-MB-231 cells were transfected with pcDNA-ZBTB16 alone or in combination with sh-ANXA7. We found that ZBTB16 overexpression obviously promoted ANXA7 expression, while transfection of MDA-MB-231 cells with sh-ANXA7 decreased ANXA7 expression (Figure 6A,B). Cyclin B1 expression was inhibited by ZBTB16 overexpression but promoted by ANXA7 knockdown (Figure 6A). Furthermore, ZBTB16 overexpression inhibited proliferation (Figure 6B) and invasion (Figure 6C) in MDA-MB-231 cells, while ANXA7 knockdown reversed these effects. In addition, ZBTB16 overexpression induced cell cycle arrest at the G2/M phase (Figure 6D) and promoted apoptosis (Figure 6E) in MDA-MB-231 cells, which was

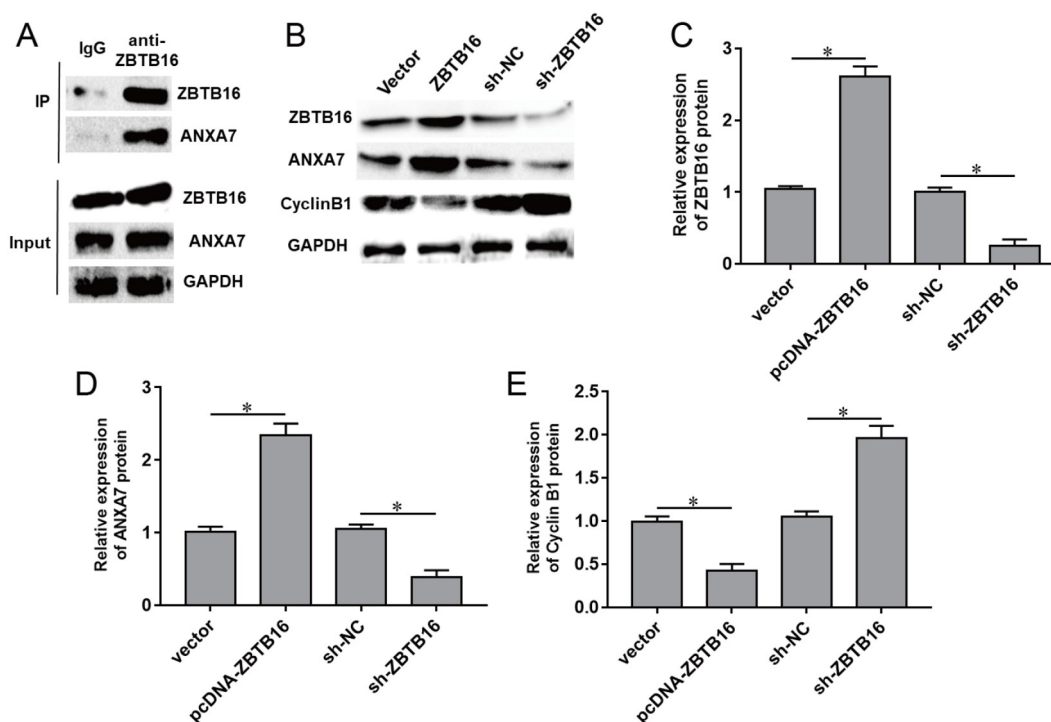


Figure 5. ZBTB16 interacts with ANXA7 and positively regulates ANXA7 expression (A) The interaction between the ZBTB16 protein and the ANXA7 protein was verified by co-IP assay. (B–E) pcDNA-ZBTB16 (1.2 µg/mL), sh-ZBTB16 (1 mL, 10¹⁰ PFU/mL), and their negative controls were transfected into MDA-MB-231 cells. Western blot analysis was used to measure the protein expressions of ZBTB16, ANXA7 and Cyclin B1 in MDA-MB-231 cells. Data are presented as the mean±SD from at least three replicate experiments. **P*<0.01.

abolished by ANXA7 knockdown. These results demonstrated that ZBTB16 inhibited breast cancer cell malignancies by regulating the ANXA7/Cyclin B1 axis. Moreover, as expected, overexpression of UHRF1 suppressed ANXA7 expression and increased the level of cyclin B1, while shUHRF1 promoted ANXA7 expression and decreased the level of cyclin B1 (Supplementary Figure S3), suggesting that UHRF1 promoted breast cancer cell malignancies by regulating the ZBTB16-mediated ANXA7/Cyclin B1 axis.

UHRF1 knockdown inhibits breast cancer tumor growth in xenograft mice

The effect of UHRF1 on breast cancer progression was further verified in xenograft tumor mice *in vivo*. First, UHRF1 was knocked down in the human normal breast epithelial cell line MCF10A to observe its safety in normal cells. Our results showed that UHRF1 knockdown had no obvious effect on cell apoptosis or proliferation in MCF10A cells, preliminarily suggesting that targeting UHRF1 is safe *in vitro* (Supplementary Figure S4). MDA-MB-231 cells transfected with sh-NC or sh-UHRF1 were injected subcutaneously into nude mice. The tumor volumes and weights in the sh-UHRF1 group were significantly lower than those in the sh-NC group (Figure 7A–C). Moreover, IHC and western blot analyses revealed that the protein expression level of UHRF1 was decreased and that the protein expression levels of ZBTB16 and ANXA7 were increased in the tumor tissues of the sh-UHRF1 group compared with those in the sh-NC group (Figure 7D). Collectively, our results demonstrated that UHRF1 knockdown inhibited breast cancer progression *in vivo*.

Discussion

Increasing evidence has shown that UHRF1 is upregulated in a

variety of cancer types, including prostate, gastric, lung and colorectal carcinomas [17]. Additionally, UHRF1 overexpression plays crucial roles in regulating proliferation, migration, invasion, cell cycle arrest and apoptosis in cancer cells [4,5]. Existing evidence has revealed that UHRF1 is upregulated in breast cancer and that UHRF1 promotes the proliferation, invasion and migration of breast cancer cells [9]. Similarly, our study confirmed that UHRF1 was upregulated in breast cancer tissues and cell lines. Moreover, UHRF1 knockdown significantly inhibited breast cancer cell proliferation and invasion, induced G2/M cell cycle arrest and apoptosis in breast cancer cells, and reduced tumor growth *in vivo*. Upregulation of UHRF1 expression usually promotes tumorigenesis by triggering aberrant patterns of DNA methylation and subsequently silences tumor suppressor genes. Silencing of UHRF1 inhibited esophageal squamous cell carcinoma cell growth by inhibiting the methylation of PTEN and subsequently upregulating its expression [18]. Moreover, UHRF1 is closely related to the pathogenesis of breast cancer by regulating the transcription of BRCA1 via the induction of DNA methylation and histone modifications [19]. Our study revealed that UHRF1 promotes breast cancer progression by reducing ZBTB16 expression by recruiting DNMT1 to promote ZBTB16 promoter methylation.

Previous studies have shown that ZBTB16 is downregulated and acts as a tumor suppressor gene in multiple cancer types, such as hepatocellular carcinoma [13], primary malignant melanoma [14], and prostate cancer [20]. Epigenetic modification of ZBTB16 through DNA methylation was found to be strongly related to cancer progression. ZBTB16 downregulation was partially correlated with promoter hypermethylation in non-small cell lung cancers, and overexpression of ZBTB16 inhibited proliferation and

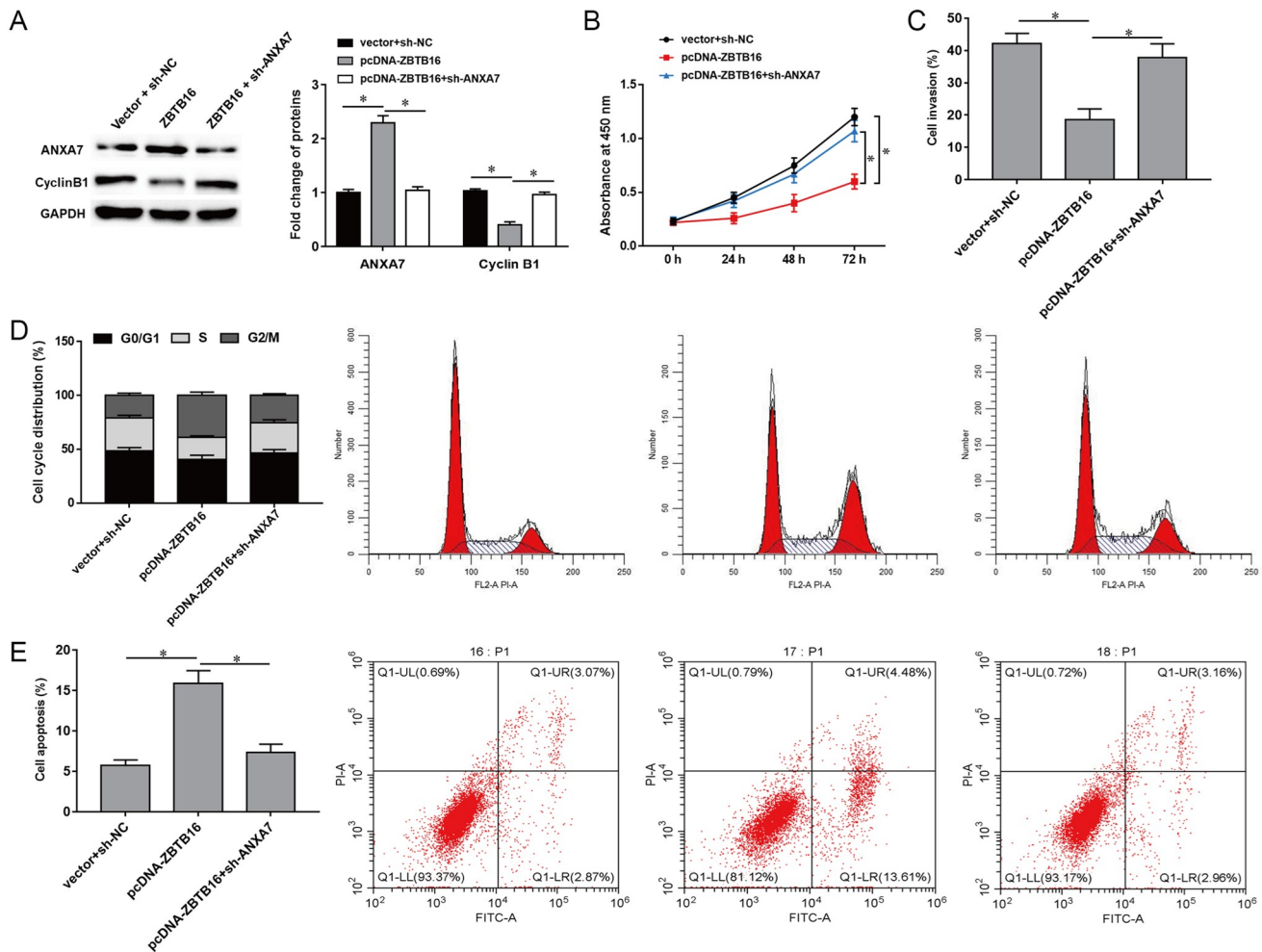


Figure 6. ZBTB16 induces cell cycle arrest and apoptosis in breast cancer cells by regulating the ANXA7/cyclin B1 axis. MDA-MB-231 cells were transfected with pcDNA-ZBTB16 (1.2 $\mu\text{g/mL}$) alone or in combination with sh-ANXA7 (1 mL, 10^{10} PFU/mL). (A) The protein expressions of ANXA7 and Cyclin B1 were measured by western blot analysis at 48 h posttransfection. (B) Cell proliferation was detected by CCK-8 assay. (C) Transwell assays were used to detect cell invasion. (D) Cell cycle distribution was analyzed by flow cytometry. (E) Cell apoptosis was measured by flow cytometry. Data are presented as the mean \pm SD from at least three replicate experiments. * $P < 0.01$.

induced apoptosis [21]. Furthermore, it was reported that down-regulated ZBTB16 expression in breast cancer cell lines is correlated with promoter hypermethylation, and ZBTB16 overexpression inhibited proliferation, invasion and migration and induced G2/M phase arrest and apoptosis *in vitro* [15]. Interestingly, our study revealed that UHRF1 reduced ZBTB16 expression by promoting ZBTB16 promoter methylation by recruiting DNMT1 in breast cancer cells. ZBTB16 knockdown promoted proliferation and migration and attenuated G2/M phase arrest and apoptosis in breast cancer cells, indicating that UHRF1 promoted breast cancer progression via epigenetic modification of ZBTB16.

Annexin A7 (ANXA7), also known as synexin, is a member of the group A annexin family. It is located on human chromosome 10q21, where multiple potential tumor suppressor genes exist. Accumulating evidence has shown that ANXA7 functions as a tumor suppressor gene in glioblastoma, melanoma and prostate cancer. Controversially, ANXA7 was also found to promote the occurrence and development of liver cancer, gastric cancer and colorectal cancer [22]. The mRNA and protein levels of ANXA7 were significantly lower in breast cancer tissues than in normal breast

tissues, and higher ANXA7 expression was associated with better clinical features and prognosis in breast cancer patients [23]. Moreover, Chinese propolis exerts its antitumor effects on breast cancer cells through the upregulation of ANXA7 level [24]. The above information indicated that ANXA7 may have tumor suppressive effects on breast cancer. Consistently, our study revealed that ANXA7 could interact with ZBTB16 and was positively regulated by ZBTB16, and ANXA7 knockdown inhibited cell cycle arrest at the G2/M phase and cell apoptosis in breast cancer. These findings are similar to the effects of ANXA7 knockdown on cell apoptosis and G2/M cell cycle in nasopharyngeal carcinoma [25]. Additionally, Cyclin B1 is known to be involved in the regulation of G2/M cell cycle [26]. We further revealed that ANXA7 negatively regulates the expression of Cyclin B1. ZBTB16 induced cell cycle arrest and apoptosis by regulating the ANXA7/Cyclin B1 axis.

Taken together, our findings suggested that UHRF1 was upregulated in breast cancer tissues and cell lines. Knockdown of UHRF1 significantly inhibited proliferation and invasion, induced G2/M cell cycle arrest and apoptosis in breast cancer cells, and reduced xenograft tumor growth *in vivo*. Mechanistically, UHRF1

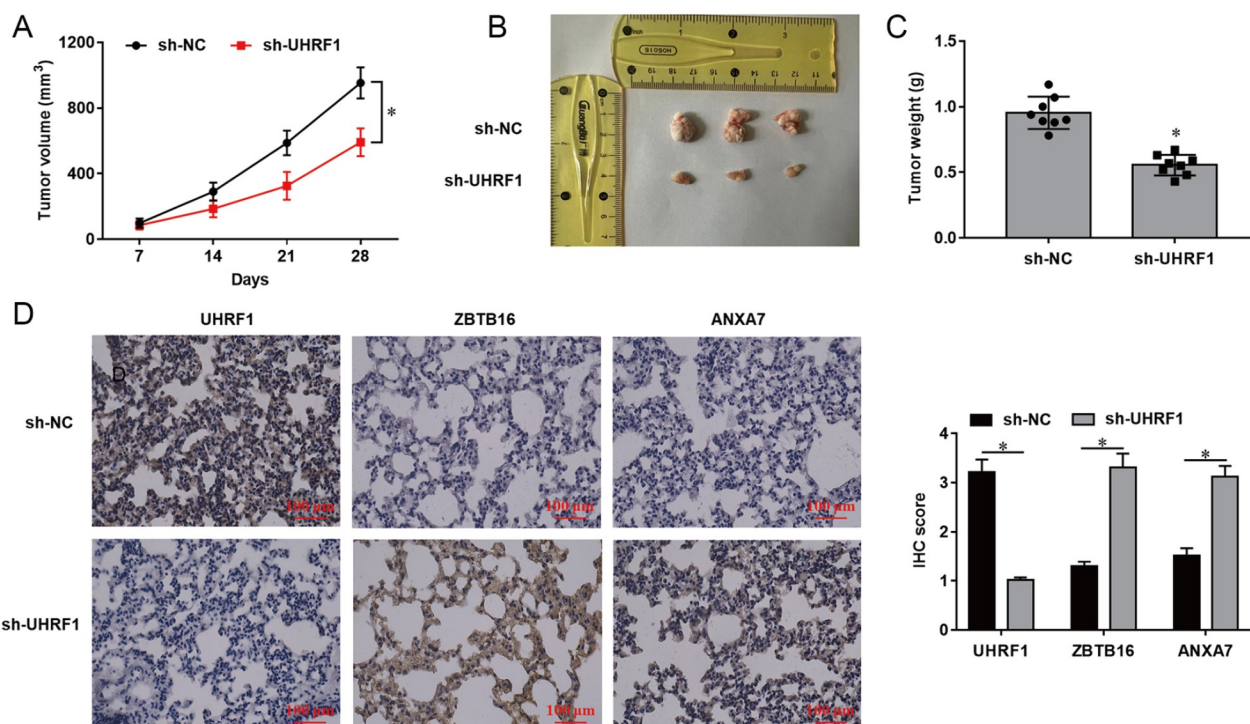


Figure 7. UHRF1 knockdown inhibits breast cancer tumor growth in xenograft mice BALB/c nude mice were randomly divided into two groups: the sh-NC group and the sh-UHRF1 group ($n=8$ per group). MDA-MB-231 cells (2×10^6 , 0.2 mL) transfected with sh-NC or sh-UHRF1 (10^{12} PFU/mL) were injected subcutaneously into the right axilla of mice. (A) Tumor volumes were measured every 7 days for 28 consecutive days after injection. (B) Representative tumor images. (C) Tumor weights were measured after euthanasia. (D) The protein expressions of UHRF1, ZBTB16 and ANXA7 in tumor tissues were detected by immunohistochemistry. Data are presented as the mean \pm SD from at least three replicate experiments. $*P < 0.01$.

negatively regulates ZBTB16 expression through DNA methylation and subsequently regulates the ZBTB16-mediated ANXA7/cyclin B1 axis. Our study may provide a molecular mechanism and potential therapeutic target for breast cancer treatment.

Supplementary Data

Supplementary data is available at *Acta Biochimica et Biophysica Sinica* online.

Funding

This work was supported by the grants from the Science and Technology Project of Shaanxi Province (No. 2022SF-496), the Key Research and Development Program of Shaanxi Province (No. 2022SF-213), the Funds of the Second Affiliated Hospital of Xi'an Jiaotong University for Scientists (No. RC (GG201807)), the Funds of the Second Affiliated Hospital of Xi'an Jiaotong University (Nos. YJ (ZYTS)2019012 and 2020YJ(ZYTS) 226], the Xinrui Cancer Research Support Program (No. cphcf-2022-231), and The Medical Research Developing Funds (No. KM228009).

Conflict of Interest

The authors declare that they have no conflict of interest.

References

- Siegel RL, Miller KD, Jemal A. Cancer statistics, 2018. *CA Cancer J Clin* 2018, 68: 7–30
- Liu H, Ye H. Screening of the prognostic targets for breast cancer based co-expression modules analysis. *Mol Med Rep* 2017, 16: 4038–4044
- Merino Bonilla JA, Torres Tabanera M, Ros Mendoza LH. Breast cancer in the 21st century: from early detection to new therapies. *Radiologia* 2017, 59: 368–379
- Li Q, Chu Z, Geng S. UHRF1 knockdown attenuates cell growth, migration, and invasion in cutaneous squamous cell carcinoma. *Cancer Invest* 2021, 39: 84–97
- Liu X, Ou H, Xiang L, Li X, Huang Y, Yang D. Elevated UHRF1 expression contributes to poor prognosis by promoting cell proliferation and metastasis in hepatocellular carcinoma. *Oncotarget* 2017, 8: 10510–10522
- Hahm JY, Park JW, Kang JY, Park J, Kim CH, Kim JY, Ha NC, *et al.* Acetylation of UHRF1 regulates hemi-methylated DNA binding and maintenance of genome-wide DNA methylation. *Cell Rep* 2020, 32: 107958
- Kim MJ, Lee HJ, Choi MY, Kang SS, Kim YS, Shin JK, Choi WS. UHRF1 induces methylation of the TXNIP promoter and down-regulates gene expression in cervical cancer. *Molecules Cells* 2021, 44: 146–159
- Zhou L, Shang Y, Jin Z, Zhang W, Lv C, Zhao X, Liu Y, *et al.* UHRF1 promotes proliferation of gastric cancer via mediating tumor suppressor gene hypermethylation. *Cancer Biol Ther* 2015, 16: 1241–1251
- Li XL. Exogenous expression of UHRF1 promotes proliferation and metastasis of breast cancer cells. *Oncol Rep* 2012, 28: 375–383
- Yan F, Tan XY, Geng Y, Ju HX, Gao YF, Zhu MC. Inhibition effect of siRNA-downregulated UHRF1 on breast cancer growth. *Cancer BioTher Radiopharms* 2011, 26: 183–189
- Kolesnichenko M, Vogt PK. Understanding PLZF: two transcriptional targets, REDD1 and smooth muscle α -actin, define new questions in growth control, senescence, self-renewal and tumor suppression. *Cell Cycle* 2011, 10: 771–775
- Xiao GQ, Unger P, Yang Q, Kinoshita Y, Singh K, McMahon L, Nastiuk K, *et al.* Loss of PLZF expression in prostate cancer by immunohistochemistry correlates with tumor aggressiveness and metastasis. *PLoS One* 2015,

- 10: e0121318
13. Hui AWH, Lau HW, Cao CY, Zhou JW, Lai PBS, Tsui SKW. Down-regulation of PLZF in human hepatocellular carcinoma and its clinical significance. *Oncol Rep* 2015, 33: 397–402
 14. Cheung M, Pei J, Pei Y, Jhanwar SC, Pass HI, Testa JR. The promyelocytic leukemia zinc-finger gene, PLZF, is frequently downregulated in malignant mesothelioma cells and contributes to cell survival. *Oncogene* 2010, 29: 1633–1640
 15. He J, Wu M, Xiong L, Gong Y, Yu R, Peng W, Li L, *et al.* BTB/POZ zinc finger protein ZBTB16 inhibits breast cancer proliferation and metastasis through upregulating ZBTB28 and antagonizing BCL6/ZBTB27. *Clin Epigenet* 2020, 12: 82
 16. Bronner C, Alhosin M, Hamiche A, Mousli M. Coordinated dialogue between UHRF1 and DNMT1 to ensure faithful inheritance of methylated DNA patterns. *Genes* 2019, 10: 65
 17. Patnaik D, Estève PO, Pradhan S. Targeting the SET and RING-associated (SRA) domain of ubiquitin-like, PHD and ring finger-containing 1 (UHRF1) for anti-cancer drug development. *Oncotarget* 2018, 9: 26243–26258
 18. Hui B, Pan S, Che S, Sun Y, Yan Y, Guo J, Gong T, *et al.* Silencing UHRF1 enhances radiosensitivity of esophageal squamous cell carcinoma by inhibiting the PI3K/Akt/mTOR signaling pathway. *Cancer Manag Res* 2021, 13: 4841–4852
 19. Jin W, Chen L, Chen Y, Xu S, Di G, Yin W, Wu J, *et al.* UHRF1 is associated with epigenetic silencing of BRCA1 in sporadic breast cancer. *Breast Cancer Res Treat* 2010, 123: 359–373
 20. Jin Y, Nenseth HZ, Saatcioglu F. Role of PLZF as a tumor suppressor in prostate cancer. *Oncotarget* 2017, 8: 71317–71324
 21. Wang X, Wang L, Guo S, Bao Y, Ma Y, Yan F, Xu K, *et al.* Hypermethylation reduces expression of tumor-suppressor PLZF and regulates proliferation and apoptosis in non-small-cell lung cancers. *FASEB J* 2013, 27: 4194–4203
 22. Guo C, Liu S, Greenaway F, Sun MZ. Potential role of annexin A7 in cancers. *Clinica Chim Acta* 2013, 423: 83–89
 23. Huang Y, Wang H, Yang Y. Annexin A7 is correlated with better clinical outcomes of patients with breast cancer. *J Cell Biochem* 2018, 119: 7577–7584
 24. Xuan H, Li Z, Yan H, Sang Q, Wang K, He Q, Wang Y, *et al.* Antitumor activity of chinese propolis in human breast cancer MCF-7 and MDA-MB-231 cells. *Evid Based Complement Alternat Med* 2014, 2014: 280120
 25. Gui SJ, Ding RL, Wan YP, Zhou L, Chen XJ, Zeng GQ, He CZ. Knockdown of annexin VII enhances nasopharyngeal carcinoma cell radiosensitivity in vivo and in vitro. *Cancer Biomark* 2020, 28: 129–139
 26. Petrachkova T, Wortinger LA, Bard AJ, Singh J, Warga RM, Kane DA. Lack of Cyclin B1 in zebrafish causes lengthening of G2 and M phases. *Dev Biol* 2019, 451: 167–179